SEISMIC RESPONSE OF FRAMED MODEL FOR HIGH-RISE RC BUILDINGS IN JAPAN

T. Akita, N. Izumi, M. Yasui, M. Kawamura and M. Sakamoto
Chiba University, Japan

SUMMARY:
In this paper, framed models are constructed based on structural planning and structural characteristics of the existing high-rise RC buildings, then time history response analysis is conducted and the seismic responses are examined. The purpose of this paper is to grasp the basic seismic capacity of the existing high-rise RC buildings. Three framed models are constructed in each design phase, thus nine framed models are constructed in total. Time history response analysis is conducted by the constructed framed model and the seismic responses are examined. As a result, in every designed generation, maximum story drift angle of framed models agreed with distribution of maximum story drift angle derived from the existing high-rise RC buildings' database. Moreover, the results showed that the damages of the existing high-rise RC buildings due to earthquake are different among the designed generations because of differences of material strength and structural planning.

Keywords: Reinforced concrete, High-rise building, Time history response analysis, Seismic capacity

1. INTRODUCTION

So far, more than 500 high-rise RC buildings were built in Japan1. However, the structural characteristics of these existing high-rise RC buildings differ depending on the designed phases. In addition, seismic capacity of the existing high-rise RC buildings is not grasped. It is necessary to grasp the seismic capacity of the existing high-rise RC buildings not only to understand the present situation but also to enhance the earthquake resistance capacity of high-rise RC buildings.

The purpose of this paper is to grasp the basic seismic capacity of the existing high-rise RC buildings. First, framed models are constructed based on structural planning and structural characteristics of the existing high-rise RC buildings. 555 high-rise RC buildings designed from 1971 to 2009 were collected and classified into the three design phases by means of the development of structural techniques on high-rise RC buildings as shown in figure 1. Second, time history response analysis is conducted and the seismic responses are examined.

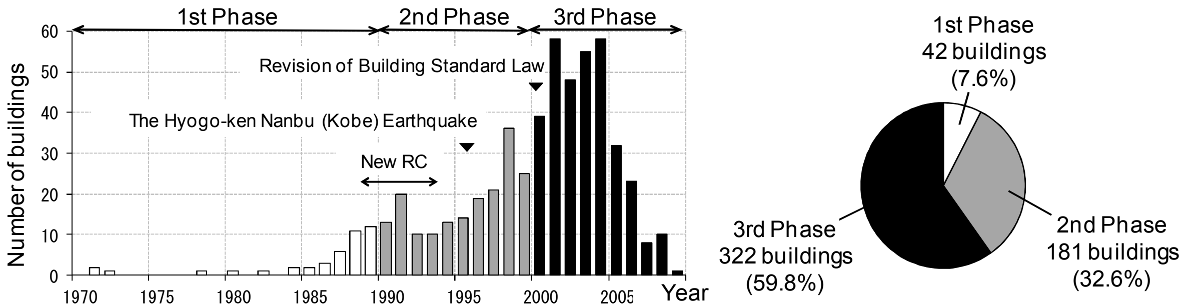

(a) Transition of number of buildings (b) Rate of three design phases

Figure 1. Structural design phases for high-rise RC buildings

2. SEISMIC CAPACITY DISTRIBUTION OF EXISTING HIGH-RISE RC BUILDINGS

The second chapter describes the seismic capacity of existing high-rise RC buildings based on the database. Natural period, base shear coefficient and seismic response (maximum story drift angle due to level 1 and level 2 earthquakes) are taken up as the values showing the seismic capacity.

2.1. Distribution of Natural Period and Shear Coefficient

Figure 2 shows the distribution of number of buildings for the coefficient (T1/H) of relationship between natural period (T1: second) and building height (H: meter) of high-rise RC building. Where, T1 is average of the X and Y direction. It is found that the coefficient (T1/H) has gradually increased according to the design phase progress, because span length and thickness of floor slab of housing room increased. In the third phase, half of the buildings show that the coefficient (T1/H) is greater than or equal to 0.02.

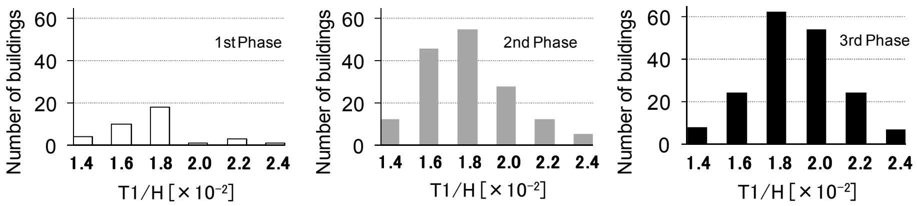

	Average value (T1/H)
1st Phase	0.0185
2nd Phase	0.0191
3rd Phase	0.0200
All Phase	0.0197

Figure 2. Distribution of number of buildings for the coefficient (T1/H) in three design phases

Figure 3 shows the distribution of number of buildings for the value (C_BxT1) which multiplied base shear coefficient (C_B) by T1. The value (C_BxT1) means the index of capacity of damage limit state considering the seismic force. It indicates that the value (C_BxT1) has gradually decreased according to the design phase progress. Particularly, the decreasing is remarkable in the third phase. In the third phase, half of the buildings show that the value (C_BxT1) is from 0.14 to 0.18.

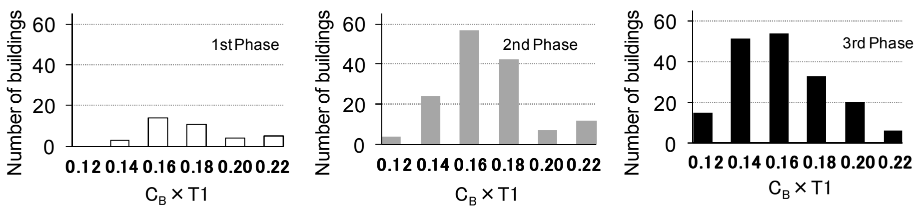

	Average value (C_B×T1)
1st Phase	0.189
2nd Phase	0.180
3rd Phase	0.172
All Phase	0.177

Figure 3. Distribution of number of buildings for CBxT1 in three design phases

2.2. Distribution of Seismic Response

Figure 4 shows the distribution of number of buildings for maximum story drift angle (R1) due to the level 1 earthquake ground motions. There are three earthquake motions (El Centro NS, Taft EW, and Hachinohe NS) in figure 4. Almost all the buildings show that the value of R1 is less than 1/200 radian which is the rough limit value of design in the level 1 earthquake. In addition, the shape of distribution in the second design phase is similar to that of the third design phase.

It is found that the maximum story drift angle (R1) occurred in many buildings when Taft EW ground motion is inputted in the second design phase and the third design phase. It isn't clear in the first design phase because of shortage of the data. Because the response due to the level 1 earthquake ground motion is almost elastic, the response may be increased easily due to Taft EW in which short periods are dominant.

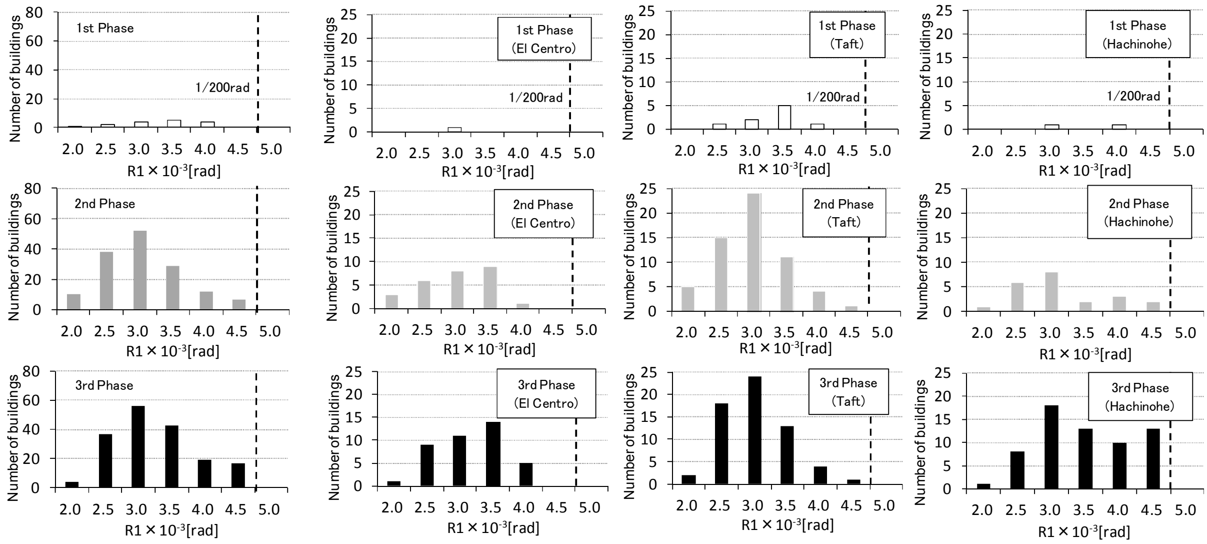

(a) Whole distribution (b) Distribution for every earthquake motions

Figure 4. Distribution of number of buildings for R1 in three design phases

Figure 5 shows the distribution of number of buildings for maximum story drift angle (R2) due to the level 2 earthquake ground motions. There are three earthquake motions (El Centro NS, Taft EW, and Hachinohe NS) in figure 5. In the third design phase, there are many buildings around 1/100 radian which is the rough limit value of design in the level 2 earthquake. Moreover, it is found that the number of buildings increase near 1/100 radian according to the progress of design phase.

The distribution of number of buildings for maximum story drift angle (R2) is different from the distribution for R1. In every design phase, the number of buildings in which the maximum story drift angle (R2) occurred due to Taft EW ground motion is less than the number of buildings in which the maximum story drift angle (R1) occurred due to Taft EW ground motion. On the other hand, the maximum story drift angle (R2) occurred in many buildings when El Centro NS and Hachinohe NS ground motion are inputted in the second design phase and the third design phase.

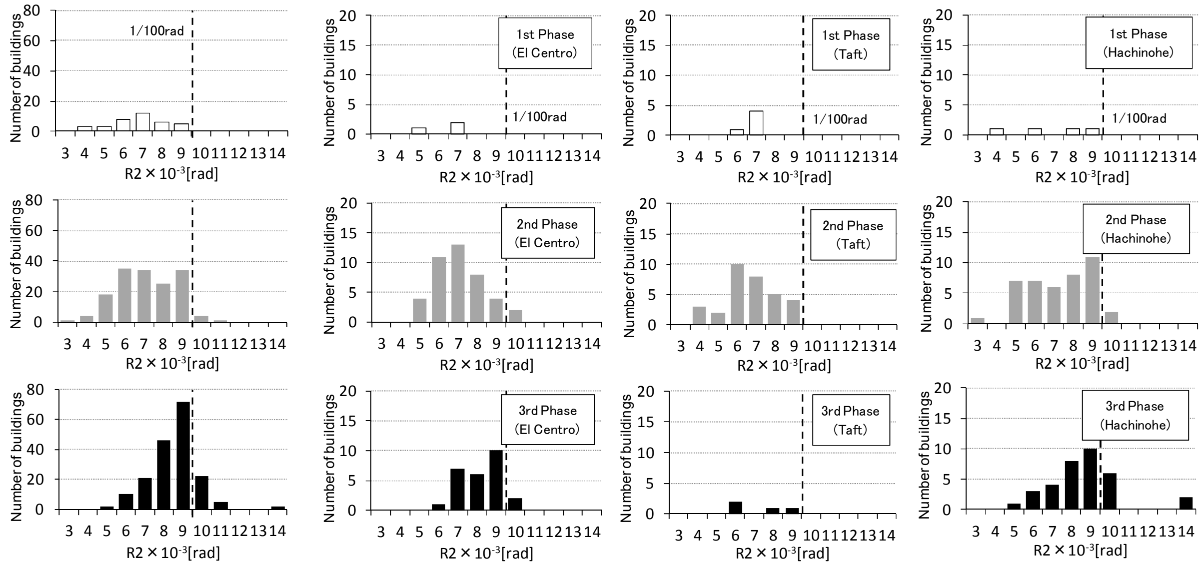

(a) Whole distribution (b) Distribution for every earthquake motions

Figure 5. Distribution of number of buildings for R2 in three design phases

3. FLAMED MODEL

In the third chapter, framed models are constructed based on structural planning and structural characteristics of the existing high-rise RC buildings. The structural planning and the structural characteristics were obtained from existing research conducted by the authors.

3.1. Outline of Flamed Model

Table 1 summarizes the specifications of the framed models, and Figure 6 shows the sketch of framing plan and elevation of framed models. Three framed models are constructed in each designed phases, thus nine framed models are constructed in total. In the time history analysis, we have eighteen analytical cases because we can use framed model into both direction X and Y. Constructed framed models correspond with the structural planning and the structural characteristics of each generation derived from analysis of the existing high-rise RC buildings' data base.

Framed models of the first design phase are 20-stories model (1G20), 25-stories model (1G25), and 30-stories model (1G30). Their typical story height is 2.95m and their span lengths are 4.5m and 5.0m. The maximum value of design compressive strength of concrete (Fc) is 42N/mm^2 and the maximum value of tensile yield strength of longitudinal bar is 390N/mm^2.

Framed models of the second design phase are 20-stories model (2G20), 30-stories model (2G30), and 40-stories model (2G40). Their typical story height is 3.0m and their span lengths are 5.0m and 6.0m. The maximum value of design compressive strength of concrete (Fc) is 60N/mm^2 and the maximum value of tensile yield strength of longitudinal bar is 490N/mm^2.

Framed models of the third design phase are 20-stories model (3G20), 30-stories model (3G30), and 40-stories model (3G40). Their typical story height is 3.1m and their span lengths are 6.0m and 6.5m. The maximum value of design compressive strength of concrete (Fc) is 70N/mm^2 and the maximum value of tensile yield strength of longitudinal bar is 490N/mm^2.

Table 1. Specifications of Framed Models

Design pahse	1st Phase						2nd Phase						3rd Phase					
Model	1G20		1G25		1G30		2G20		2G30		2G40		3G20		3G30		3G40	
Direction	X	Y	X	Y	X	Y	X	Y	X	Y	X	Y	X	Y	X	Y	X	Y
Height (m)	60.75		75.5		90.25		61.7		91.7		121.7		63.6		94.6		125.6	
Building stories	20		25		30		20		30		40		20		30		40	
Typical story height (m)	2.95		2.95		2.95		3		3		3		3.1		3.1		3.1	
Typical floor area (m^2)	675		787.5		945		600		900		1050		585		936		1170	
Typical floor area supported by a column (m^2)	22.5		22.5		22.5		30.0		30.0		30.0		39.0		39.0		39.0	
Span length (m)	4.5	5	4.5	5	4.5	5	5	6	5	6	5	6	6	6.5	6	6.5	6	6.5
Number of spans	6	5	7	5	7	6	5	4	6	5	7	5	5	3	6	4	6	5
Aspect ratio	2.25	2.43	2.40	3.02	2.87	3.01	2.47	2.57	3.06	3.06	3.48	4.06	2.12	3.26	2.63	3.64	3.49	3.86
Design compressive strength of concrete [Fc] (N/mm^2)※1	36		36		42		36		48		60		42		54		70	
Tensile yield strength of longitudinal bar (N/mm^2)※2	390		390		390		390		490		490		490		490		490	
Average weight (kN/m^2)※3	14.5[11.2]		14.3[11.3]		14.8[11.9]		15.5[11.8]		14.9[11.9]		14.4[11.7]		15.4[11.6]		14.3[11.4]		13.4[10.9]	
Natural period [T1] (sec)	1.11	1.12	1.36	1.36	1.65	1.66	1.17	1.17	1.69	1.71	2.27	2.35	1.27	1.28	1.79	1.92	2.34	2.40
Base shear coefficient [C_B]	0.163		0.130		0.113		0.145		0.105		0.074		0.134		0.090		0.068	

※1 : The maximum value of design compressive strength of used concrete.

※2 : The maximum value of tensile yield strength of used longitudinal bars.

※3 : The value calculated from typical floor weight divided by typical floor area which excluded balcony.
(The value inside [ ] is including balcony.)

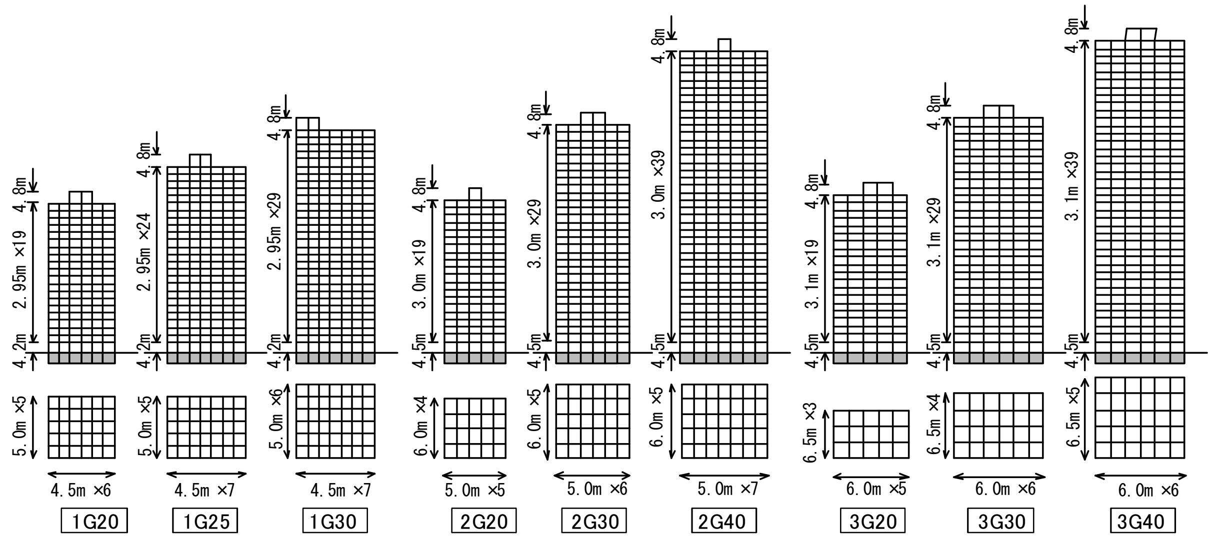

Figure 6. Sketch of framing plan and elevation of framed models

3.2. Natural Period and Shear Coefficient of Framed Model

In construction of the framed model, the target natural period of the framed model is calculated using the coefficient (T1/H) of relationship between natural period (T1) and building height (H) as shown in figure 2. The coefficient (T1/H) of the first design phase, the second phase, and the third phase is 0.0185, 0.019, and 0.020 respectively. On the other hand, the target base shear coefficient ($C_{B)}$ of the framed model is calculated using the value (C_BxT1) as shown in figure 3. The value (C_BxT1) of the first design phase, the second phase, and the third phase is 0.19, 0.18 and 0.17 respectively.

The sections of beams and columns in the framed model are determined to satisfy the target natural period. Also the sections are determined that the capacity of framed model demonstrates around 1.6 times of C_B when the representative deformation angle (R_T) is 1/100 radian as shown in figure 7. Where the representative deformation angle (R_T) is calculated at the two thirds of building's height. Furthermore, the sections are determined that the capacity of framed model demonstrates around 1.7 times of C_B when the representative deformation angle (R_T) is 1/50 radian. Unknown data, for example, floor weight, thickness of floor slab, etc., are determined by taking into account the practical design data.

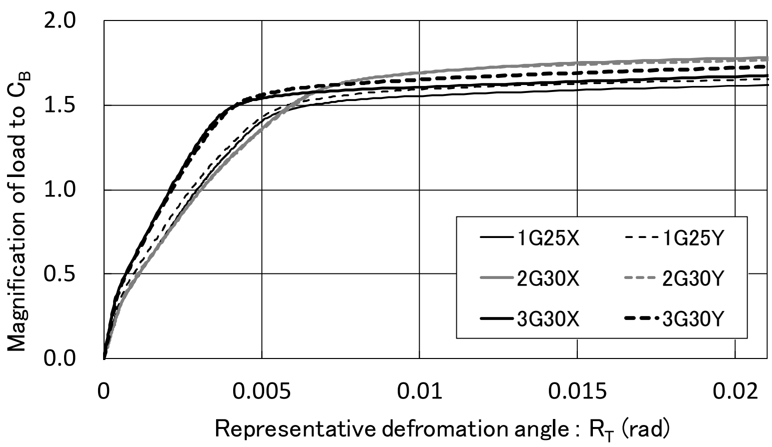

Figure 7. Relationship between base shear coefficient and representative deformation angle

4. TIME HISTORY RESOPONSE ANALYSIS OF FRAMED MODEL

The fourth chapter presents the time history response analysis of framed model which was conducted to examine the seismic capacity of existing high-rise RC buildings.

4.1. Outline of Time History Response Analysis

Three-dimensional framed model with rigid floor which considered the elasto-plastic characteristics of beam and column member is used. The framed model has the tri-linear skeleton curve for beams and columns, and the TAKEDA MODEL is applied to the hysteresis characteristics of beams and columns. Reduction index of unloading stiffness is 0.50 (for beam) or 0.40 (for column). The viscous damping in proportion to momentary stiffness is assumed and the damping factor of the first mode is 0.03.

Table 2 shows the input earthquake motions used in the time history response analysis. Three actual earthquake ground motions (El Centro NS, Taft EW, and Hachinohe NS) and one simulated earthquake ground motion which was issued by Building Center of Japan (BCJ-L2) are used. In case of using the actual earthquake ground motions, the intensity of the input earthquake ground motions is standardized by the maximum velocity so that the velocity of the level 1 earthquake ground motion is 25cm/sec and the velocity of the level 2 earthquake ground motion is 50cm/sec.

Table 2. List of Input Earthquake Ground Motions

Input earthquake ground motion			Actual earthquake			Simulated earthquake
			El Centro NS	Taft EW	Hachinohe NS	BCJ-L2
Level 1	Maximum velocity	[cm/s]	25	25	25	−
	Maximum acceleration	[cm/s^2]	254	251	166	−
Level 2	Maximum velocity	[cm/s]	50	50	50	57
	Maximum acceleration	[cm/s^2]	509	503	332	356

4.2. Result of Time History Response Analysis

Figure 8 shows the maximum response of story drift angle due to the level 1 earthquake motions and the level 2 earthquake motions, and Table 3 summarizes the maximum response of story drift angle. It can be seen that R1 is 1/300 to 1/340 radian and R2 is 1/100 to 1/160 radian in the first design phase. Also the R1 is 1/270 to 1/330 radian and R2 is 1/100 to 1/120 radian in the second design phase, and the R1 is 1/200 to 1/290 radian and R2 is 1/100 to 1/130 radian in the third design phase. The story drift angle was not increased at particular story in every framed model as shown in figure 8.

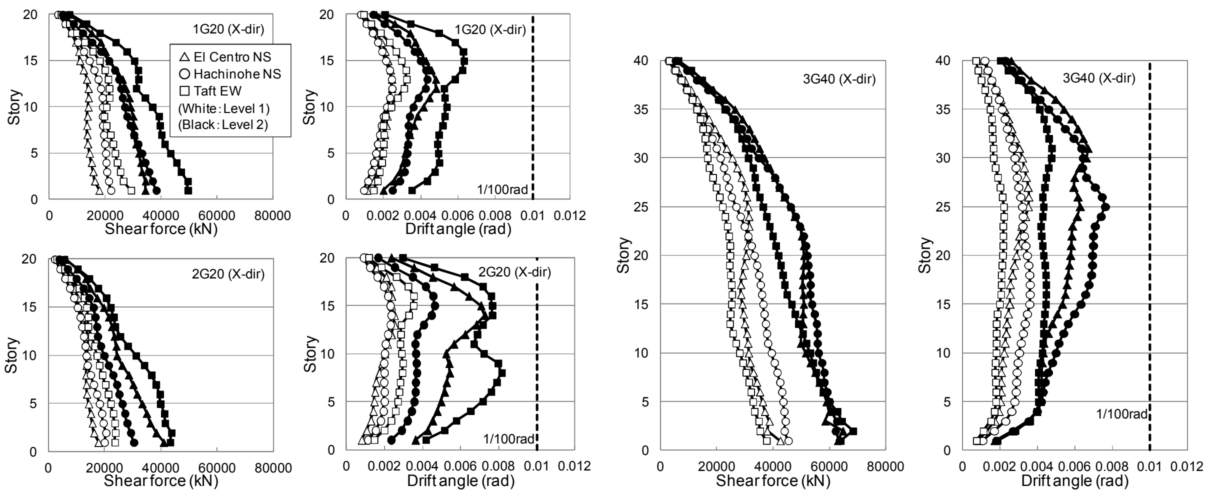

Figure 8. Maximum response of shear force and drift angle

Table 3. List of Maximum Response of Story Drift Angle

Model	Direction	Level 1			Level 2		
		Drift angle	Story	Input wave motion	Drift angle	Story	Input wave motion
1G20	X	1/310	13	Taft	1/159	15	Taft
	Y	1/323	14	Taft	1/149	16	Taft
1G25	X	1/313	19	Taft	1/140	3	El Centro
	Y	1/305	8	Taft	1/149	16	El Centro
1G30	X	1/344	21	El Centro	1/104	21	Hachinohe
	Y	1/342	21	El Centro	1/116	21	El Centro
2G20	X	1/285	16	Taft	1/123	8	Taft
	Y	1/301	15	Taft	1/125	7	Taft
2G30	X	1/301	20	El Centro	1/101	18	Hachinohe
	Y	1/335	15	El Centro	1/103	17	Hachinohe
2G40	X	1/268	28	El Centro	1/113	28	Hachinohe
	Y	1/268	28	El Centro	1/114	28	Hachinohe
3G20	X	1/254	15	Taft	1/108	14	Taft
	Y	1/290	14	Taft	1/123	14	Taft
3G30	X	1/202	15	Hachinohe	1/105	13	Hachinohe
	Y	1/206	18	Hachinohe	1/105	6	Hachinohe
3G40	X	1/276	17	Hachinohe	1/131	25	Hachinohe
	Y	1/272	28	El Centro	1/135	23	Hachinohe

5. SEISMIC CAPACITY OF FRAMED MODEL

In order to confirm the seismic capacity of the constructed framed models, the maximum story drift angle obtained by the time history response analysis is examined in comparison with the distribution of number of buildings for the maximum story drift angle (R1 and R2) based on the database. Figure 9 and figure 10 show the correspondence between framed model and database for R1 and R2. It is found that every model corresponds with the range which has large number of buildings, such as “2G20(Y)” in second phase in figure 9. Therefore, it is confirmed that constructed framed models correspond with seismic capacity of the existing high-rise RC buildings.

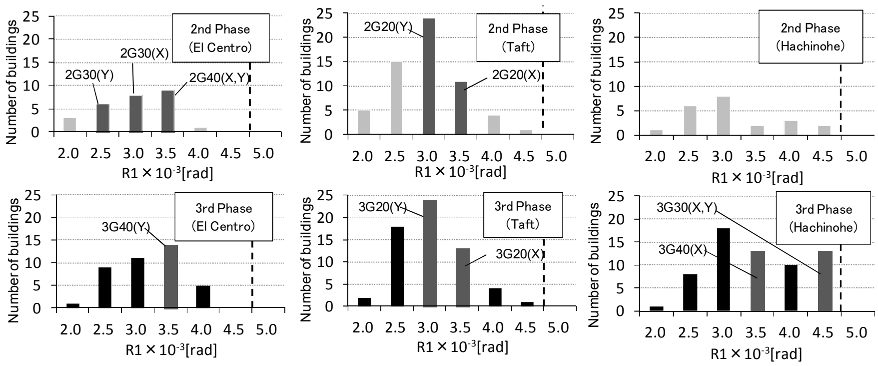

Figure 9. Correspondence between framed model and database for R1

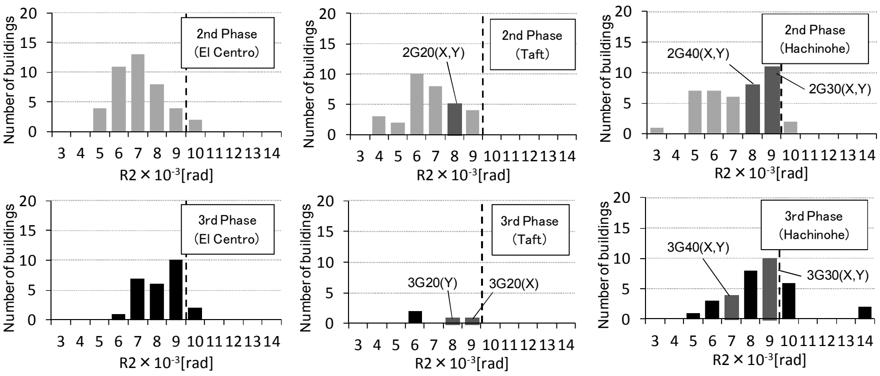

Figure 10. Correspondence between framed model and database for R2

Figure 11 shows the ductility factor of beam and maximum story drift angle due to BCJ-L2 earthquake ground motion. The gray lines mean the case which inputted the original BCJ-L2, and the black lines mean the case which inputted the amplified BCJ-L2. The maximum story drift angle reaches 1/50 radian when the amplified BCJ-L2 inputted. In the case which inputted the amplified BCJ-L2, it is found that the tendency in which the ductility factor of beam in first phase's model is greater than that in the others. The causes of this tendency are differences of material strength and structural planning.

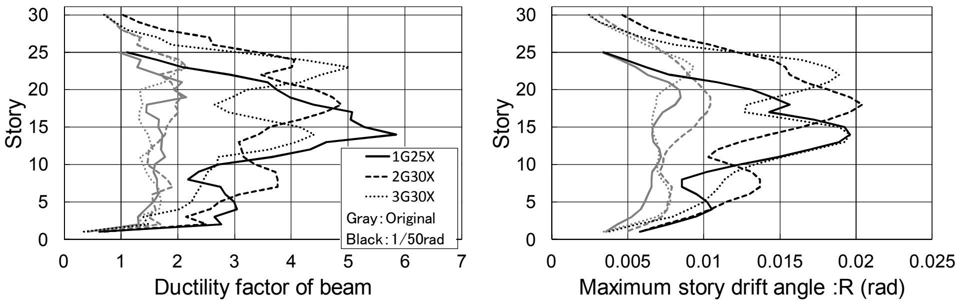

Figure 11. Ductility factor of beam and maximum story drift angle

6. CONCLUSIONS

In this paper, the framed models which represent existing high-rise RC buildings in three design phases were constructed based on the existing high-rise RC buildings' database. Then, seismic capacity of the existing high-rise building was evaluated from examination of seismic response of the framed models. The findings obtained in this study may be summarized as follows.

(1) From the database, it was shown that the maximum story drift angle R1 (story drift angle due to level 1 earthquake) occurred in many buildings when Taft EW ground motion was inputted.

(2) From the database, it was shown that the maximum story drift angle R2 (story drift angle due to level 2 earthquake) occurred in many buildings when El Centro NS or Hachinohe EW ground motions were inputted.

(3) In every design phase, maximum story drift angle of framed models agreed with distribution of maximum story drift angle derived from the existing high-rise RC buildings' database. Therefore, it was confirmed that constructed framed models correspond with the seismic capacity of the existing high-rise RC buildings.

(4) The tendency in which the ductility factor of beam in first phase's model is greater than that in the others was shown. The causes of this tendency are differences of material strength and structural planning.

AKCNOWLEDGEMENT

This paper was conducted as a part of program (No.22560556) " Evaluation of seismic performance and improvement by energy dissipation devices on existing high-rise seismic RC buildings in Japan" supported by Grants-in-Aid Scientific Research in Japan.

REFERENCES

The Building Center of Japan. (1967-2009). Building letter (in Japanese), No.1-No.525

Izumi, N., Kimura, H. and Ishikawa, Y. (2009). Structural characterisitics of high-rise reinforced concrete buildings in Japan (in Japanese). *Proceedings of Structural Engineering.* **Vol.55B**, 351-360

Akita, T., Ioi, T, Eda, T., Kurimoto, K. and Izumi, N. (2010). Structural plannning and seismic design value of existing high-rise RC buildings (in Japanese). *Proceedings of the 13 Japan Conference on Earthquake Engineering (CD-ROM)*, 3081-3086

Akita, T., Kurimoto, K. Ioi, T. and Izumi, N. (2011). Structural characteristics and frame models of exisiting high-rise RC buildings (in Japanese). *Proceedngs of Japan Concrete Institute.* **Vol.33: 2**, 925-930